JOURNAL OF MATERIAL SCIENCE 31 (1996) 3115–3121

Characterization of pre-shaped zirconia bodies for catalytic applications

L. A. BOOT*, A. J. VAN DILLEN, J. W. GEUS, F. R. VAN BUREN‡
Department of Inorganic Chemistry, Debye Institute, Utrecht University, P.O. Box 80083, 3508 TB Utrecht, The Netherlands

Literature indicates that application of zirconia in a supported dehydrogenation catalyst is viable. Textural and structural properties of commercial pre-shaped zirconia supports from various suppliers were characterized using electron microscopy, element analysis, nitrogen physisorption, mercury intrusion porosimetry and X-ray diffraction. Most zirconias are sufficiently pure (>97 %) and thermostable to be applied in supported catalysts. Specific surface areas as large as 10 $m^2 g^{-1}$ are stable at temperatures of about 850 °C. Specific surface areas up to about 30 $m^2 g^{-1}$ can be established by a thermal treatment in air at temperatures up to the operating temperatures of the dehydrogenation process. Steam treatment affects the texture differently from treatment in dry air: sintering proceeds more rapidly in the presence of steam. The preshaped supports show a porosity (about 50%) which is higher than that reported for zirconia powders with the same pore-size distribution (5%). This is advantageous, both in the catalyst preparation step and in the catalytic reaction. However, the pre-shaped supports exhibit some microporosity.

1. Introduction

The currently applied bulk iron oxide catalysts for ethylbenzene dehydrogenation suffer from a decrease in mechanical strength caused by solid-state phase transitions and from migration of the potassium promoter [1,2]. In search of an improved catalyst to replace the bulk iron oxide catalyst, research was directed to develop supported catalyst systems [3–7]. Selection criteria for a possible candidate support material included:

(i) availability as commercial pre-shaped support bodies to avoid the incorporation of a shaping step in the catalyst production. The shaping of oxidic materials to bodies of the sizes and geometric forms necessary to employ the catalyst in an industrial process is still an empirical "science", and hence usually a very complicated task. However, this effort can be avoided by using commercially available pre-shaped support bodies for preparing the supported catalyst;

(ii) thermostability and stability towards steam;

(iii) acid–base characteristics of the material;

(iv) adequate interaction with the applied active components.

The conventional catalyst supports, alumina and silica, were rejected as candidates because of their acidity and the reactivity of these oxides with potassium. Moreover, silica is somewhat volatile and shows loss of surface area in the presence of steam at high temperatures and pressures. Magnesia meets with these severe demands, so pre-shaped bodies of magnesia were used to support the active phase consisting of an iron- and potassium-containing compound. However, the reaction of magnesia to its hydroxide (brucite) at temperatures below 250 °C, during, for example, start-up or storage, might deteriorate the mechanical strength of the support bodies and give rise to microporosity [5, 6].

Zirconium dioxide (zirconia) is another candidate support material for application in dehydrogenation catalysts. Concerning the selection criteria mentioned above, some remarks regarding the a priori suitability of zirconia can be made.

The thermal stability of zirconia supports seems sufficient for application in dehydrogenation processes. Dehydrogenation catalysts do not require specific surface areas larger than 10 $m^2 g^{-1}$ [1, 8]. Because the operating temperatures lie in the range 600–650 °C, specific surface areas can be installed from 3–50 $m^2 g^{-1}$ by thermal treatments, *e.g.* [9–11]. Whether the corresponding pore structure is suited for application in dehydrogenation is less clear. Also, no examples of the use of pre-shaped support bodies have been found in the literature. The catalytic properties of zirconia itself are not expected adversely to affect the dehydrogenation reaction. The oxide is not very acidic [12]. An excessive (and unfavourable) hydrocarbon cracking activity is therefore not predicted. Moreover, the

Present address: Akzo Nobel Chemicals BV, PO Box 37650, 1030 BE Amsterdam, The Netherlands.
‡*Present address*: Dow Benelux N.V., P.O. Box 48, 4530 AA Terneuzen, The Netherlands.

0022–2461

dehydrogenation of ethylbenzene is reported to proceed over zirconia [13].

The formation of mixed compounds with the applied active elements (iron, potassium) can also be disadvantageous, as in the case of a titanium dioxide support [14]. No compounds in the Fe–Zr–O system have been observed [15], although there is some disagreement in the literature about the possible formation of a solid solution of iron oxide in zirconia with iron salt–zirconium salt co-precipitates [16–19]. However, because the supported catalysts will be prepared by application of an iron compound on to a pre-shaped support oxide, the occurrence of solid solutions is not likely: a solid solution has not been reported in the literature on Fe_2O_3/ZrO_2 catalysts [20, 21]. Furthermore, no formation of mixed compounds of zirconia with potassium under dehydrogenation conditions is expected [22–25]. Summarizing, it is expected that zirconia will fulfil the pre-set requirements.

Two studies dealing with the preparation and properties of zirconia powders as a catalyst support are known, namely, Rijnten's thesis [26] and Mercera's thesis [9]. These studies do not include investigations on the use of pre-shaped supports, or on the preparation of supported catalysts. In the present paper, the characterization of the pre-shaped supports used for developing the zirconia-supported catalysts is described. Consecutively, the chemical composition and the textural and structural properties of the supports will be dealt with. Because the application of a zirconia-supported catalyst in non-oxidative dehydrogenation requires stability of the porous zirconia support at elevated temperatures in a feed stream containing about 30 vol % steam, the influence of a thermal treatment and of steam on the support texture is also investigated. The development of zirconia-supported catalysts using pre-shaped support bodies will be described in forthcoming papers.

2. Experimental procedure

Pre-shaped zirconia bodies were obtained from various suppliers. The examined samples are presented in Table I.

To investigate the thermostability of the various supports, the materials were subjected to a treatment in air at 850 °C. The Daiichi (I) material was examined in more detail. To this end, the effect of treatment time and temperature on the textural properties was studied. To assess the influence of steam, both fresh and thermally pre-treated Daiichi (II) material was heated for 16 h at 600 °C and 700 °C in a flow of unsaturated steam (100 ml min^{-1}, 30 vol % in nitrogen). The Daiichi (I) zirconia was also subjected to hydrothermal conditions (150 °C, 4.76 bar H_2O). The treated samples were investigated using nitrogen physisorption, mercury intrusion porosimetry, electron microscopy, and XRD.

TABLE I Zirconia samples investigated in the present work

Manufacturer	Type	Shape	Size	
			(mm)	(in)
Daiichi	RSC-H[a]	Pellets	3	
Engelhard	L6132	Pellets		1/8
Norton	XZ16052	Extrudates	3	
	XZ16075	Extrudates	3	

[a] Two batches were investigated, designated batches I and II.

2.1. Chemical analysis

The chemical composition of the supports was determined using X-ray fluorescence (XRF, Philips PW1480 and Uniquant software, version 2) and/or energy dispersive analysis of x-rays (EDAX, Philips SEM505 and EDAX PV9900 System).

2.2. Electron microscopy

For transmission electron microscopy, samples were prepared by applying a few droplets of a dispersion of a finely ground catalyst ultrasonically treated in ethanol on to a holey carbon film supported by a copper grid. Samples were investigated in a Philips EM420 transmission electron microscope operated at 120 kV, primarily by bright-field techniques. Scanning electron microscopy was performed in a Philips SEM505 instrument.

2.3. Texture analysis

The specific surface areas of the bare supports were determined by nitrogen physisorption at liquid nitrogen temperature according to the BET method. A surface area of 0.162 nm^2 for a physically adsorbed nitrogen molecule was used for calculation of the BET surface area. Measurements were carried out by either dynamic physisorption (Quantasorb apparatus, Quantachrome Corp.) or static physisorption (ASAP 2400, Micromeritics); the latter technique also provides the complete adsorption and desorption isotherms from which the pore-size distribution up to 100 nm (according to the BJH method [27]) and information on the microporosity of the samples (t-plot method [27]) can be derived. Fractured samples with particle sizes of 0.50–0.85 mm were outgassed at 200 °C for 2 h prior to the measurements.

To determine the pore-size distribution over the range of pore sizes partially complementary to that measured with nitrogen physisorption, mercury intrusion porosimetry was used. Pore sizes from 4–10000 nm were determined on unfractured pellets using a Carlo Erba Porosimeter 2000. A contact angle of 141.3° and a surface energy of 480 mJ m^{-2} were used for calculation of the pore-size distribution; for application of the Washburn equation, a model comprising non-intersective and cylindrical pores was employed.

2.4. X-ray diffraction

XRD was carried out in a Philips powder diffractometer mounted on a Philips PW1140 X-ray generator

with $FeK_{\alpha 1,2}$ radiation (0.193 735 nm). Determination of the crystallite size from the X-ray line broadening was performed using the Scherrer equation

$$D = \frac{0.9\lambda}{\beta \cos(\theta)} \quad (1)$$

in which D is the crystallite diameter, λ is the X-ray wavelength, β is the pure line broadening at half height of the diffraction maximum corrected for the instrumental broadening, and θ is the Bragg angle.

The volume fraction of the monoclinic phase, V_m, for samples consisting of a mixture of crystallographic phases, was calculated according to an empirical formula suggested by Toraya *et al.* [28].

3. Results and discussion

3.1. Chemical analysis

The chemical composition of the samples, as determined by XRF and/or EDAX is represented in Table II. As can be seen in Table II, hafnium oxide is a minor contamination in all samples. The presence of hafnium could be expected, because it is also found in all zirconium sources, and is difficult to remove due to its chemical resemblance with zirconia. Another impurity is titania, which is also commonly found in zirconium ores. In the Engelhard material, a relatively large amount of alumina is also present.

3.2. Transmission electron microscopy

With transmission electron microscopy, small differences between the texture of the various zirconia supports could be observed. The Daiichi ZrO_2 consisted of small crystalline particles, which seem rather unimodal and are not appreciably clustered. The mean particle diameter was about 8–15 nm. After thermal treatment, a uniform sintering had occurred and the diameter has increased to about 15–35 nm.

The fresh Engelhard sample showed small (<5 nm) diffuse particles clustered together in agglomerates of about 100–300 nm. In a thermally treated sample, these agglomerates seemed to have densified. Small particles remained present locally, however. The clusters in the Engelhard material were also visible with SEM.

The Norton zirconia showed a unimodal particle distribution. The particle size increased uniformly from about 8 nm to about 40–50 nm upon sintering at 850 °C.

3.3. Texture analysis

All fresh supports showed type II or type IV adsorption isotherms, indicating the presence of pores with diameters ranging from 1.5–100 nm [27]. The observed hysteresis loops were all of type A (de Boer classification [27]), characteristic of cylindrical pores. The surface areas of the as-received supports calculated from nitrogen physisorption according to the BET method are represented in Table III which also gives the pore volume, mean pore radius, porosity and micropore area (according to the *t*-method [27]).

The supports are characterized by a specific surface area which is neither high ($> 200\,m^2\,g^{-1}$) nor low ($< 10\,m^2\,g^{-1}$). This intermediate surface area is typical for the zirconia supports encountered in the literature (*e.g.* [9]). The fact that the average pore radius is of the same order of magnitude as the particle size as determined from TEM, combined with the low microporosity, indicates that the support pore systems consist of the interstitial mesopores ($2 < r < 100$ nm)

TABLE III Textural parameters of fresh zirconia pre-shaped supports. SSA, specific surface area; PV, cumulative pore volume; $\langle r \rangle$ the mean pore radius; ε the porosity; S_μ the surface area in micropores

Support	SSA ($m^2\,g^{-1}$)	PV ($ml\,g^{-1}$)	$\langle r \rangle$ (nm)	ε (%)[a]	S_μ ($m^2\,g^{-1}$)
Daiichi I	40	0.25	9	59	3.4
Daiichi II	43	0.23	10.5	57	3.3
Engelhard	56	0.12	4.2	41	1.9
Norton					
XZ16052	98	0.26	5.4	60	3.6
XZ16075	48	0.23	9.8	57	3.6

[a] The porosity is calculated as follows: $\varepsilon = [PV/(PV + 1/\rho)]\ 100\%$, in which ρ is the theoretical density.

TABLE II Chemical composition (wt %) of various zirconia support bodies

Support		Daiichi I	Daiichi II	Engelhard	Norton
Method	Component	RSC-H	RSC-H	L6132	XZ16052 and 75
EDAX	ZrO_2	97.2		90.6	
	HfO_2	2.6		1.4	
	Al_2O_3			7.3	
	TiO_2	0.2		0.5	
XRF	ZrO_2	97.7	97.5		97.6
	HfO_2	1.8	1.8		1.8
	TiO_2	0.21	0.16		0.12
	Al_2O_3		0.27		
	Lanthanoids (mainly Ce)	0.26	0.27		0.33

between the primary, essentially non-porous zirconia crystallites. No significant differences are observed between the various supports, with exception of the Norton XZ16052 material: it has a specific surface area approaching $100\,m^2\,g^{-1}$ and an associated smallest average pore radius of 5.4 nm.

The evolution of the surface area as a function of the duration and of the temperature of thermal treatment is plotted for the Daiichi (I) material in Figs 1 and 2. It can be seen in Fig. 1 that the decrease in surface area has been completed after 10–16 h. Therefore, the period of time during the experiment in which the effect of the temperature was studied was kept constant at 16 h. The surface area of the Daiichi support remains stable up to temperatures of 700 °C. Above this temperature, sintering starts to proceed: the specific surface area (SSA) decreases constantly up to a temperature of 1100 °C, where only about $2\,m^2\,g^{-1}$ are left. The calculated surface area in micropores is reduced to about $1\,m^2\,g^{-1}$ after sintering. Regarding the temperatures applied in the dehydrogenation reaction (600–650 °C) and those during catalyst preparation, *i.e.* during the thermal treatment in which the dried catalyst is calcined (> 650 °C) it can be remarked that the texture of the fresh supports will be influenced at these temperatures. Stable textural characteristics can, if necessary, be pre-set by applying a thermal treatment at a sufficiently high temperature prior to catalyst preparation or the catalytic operation.

More data concerning the results of the thermal treatment of the Daiichi and other supports are

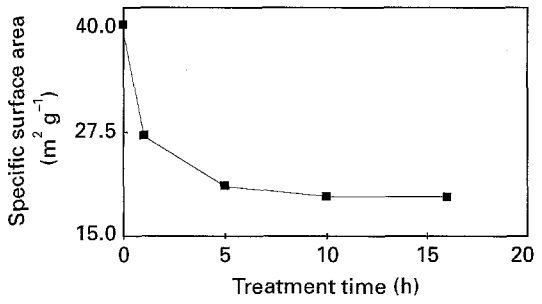

Figure 1 Evolution of the specific surface area of the Daiichi (I) material as determined with nitrogen adsorption as a function of the period of time at 850 °C in air.

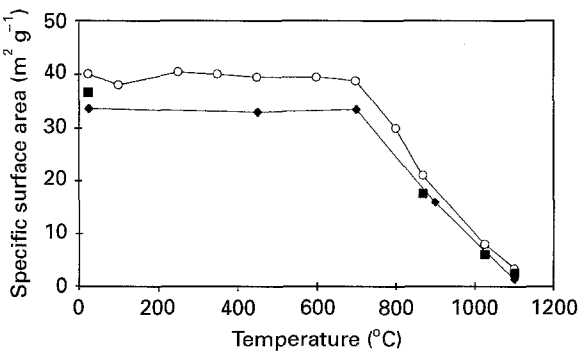

Figure 2 Evolution of the specific surface area of the Daiichi (I) material as determined with (○) nitrogen adsorption and (◆) mercury intrusion porosimetry and (■) the external surface area, S_{ext}, as a function of the temperature of thermal treatment in air for 16 h.

TABLE IV Textural parameters of zirconia supports, treated at 850 °C in air. For explanation of symbols see Table III

Support	SSA ($m^2\,g^{-1}$)	PV ($ml\,g^{-1}$)	$\langle r \rangle$ (nm)	ε (%)	S_μ ($m^2\,g^{-1}$)
Daiichi I	21.0	0.20	24	54	3.4
Daiichi II	22.2	0.18	16	51	4.4
Engelhard	20.0	0.10	10	37	2.6
Norton XZ16052	21.8	0.16	15	48	3.4
XZ16075	21.9	0.17	16	50	4.2

presented in Table IV. From the difference between the specific surface areas after thermal treatment as measured by nitrogen adsorption and by mercury porosimetry, it can be deduced that a considerable fraction of the pores in the zirconia are smaller than 4 nm, *i.e.* the smallest pore diameter measured with the mercury-intrusion experiments. Indeed, in Tables III and IV the surface areas present in micropores ($r < 2$ nm) are reported to be about $3\,m^2\,g^{-1}$ or higher for all zirconias. Therefore, the so-called external surface area, S_{ext}(= SSA-S_μ) has also been plotted in Fig. 2. This surface area is in reasonable agreement with the values obtained with porosimetry. This explains the discrepancy between the BET surface area and the surface area calculated from mercury intrusion. Next to this, it can be noted that at high temperatures (> 1000 °C) the micropores seem to be eliminated.

After thermal treatment, the various zirconia supports do not differ from each other in the resulting BET or micropore surface area, but the pore structure and associated porosity show a different behaviour. The Daiichi and Norton materials maintain comparable and fairly high porosity values. The Norton XZ16052 now displays a texture which is similar to the Daiichi supports. Up to 850 °C, no extensive sintering leading to a low porosity and densification is observed for these materials. This is in line with the results of Mercera and co-workers [9, 10]. The moderate sintering is characteristic for sintering proceeding via a solid-state diffusion process. The pore structure of the Engelhard ZrO_2 collapses more severely under the imposed thermal treatment. This may be related to the presence of the tetragonal phase in the sample (cf. XRD): sintering is accompanied by the t–m phase transition, possibly leading to an increased apparent density. With TEM, this densification was also observed.

As stated, mercury intrusion porosimetry was performed on the Daiichi samples to study the distribution of pores larger than 100 nm. Pore-size distribution curves are presented in Figs 3 and 4. Again, the evolution versus temperature was studied; the influence on the specific surface area as determined by porosimetry was already presented in Fig. 2.

The pore-size distributions of batches I and II of the Daiichi material do not differ greatly, but it must be noted that batch I has considerably more large macropores (> 1000 nm). Its pore-size distribution therefore seems more bi-modal. Upon thermal

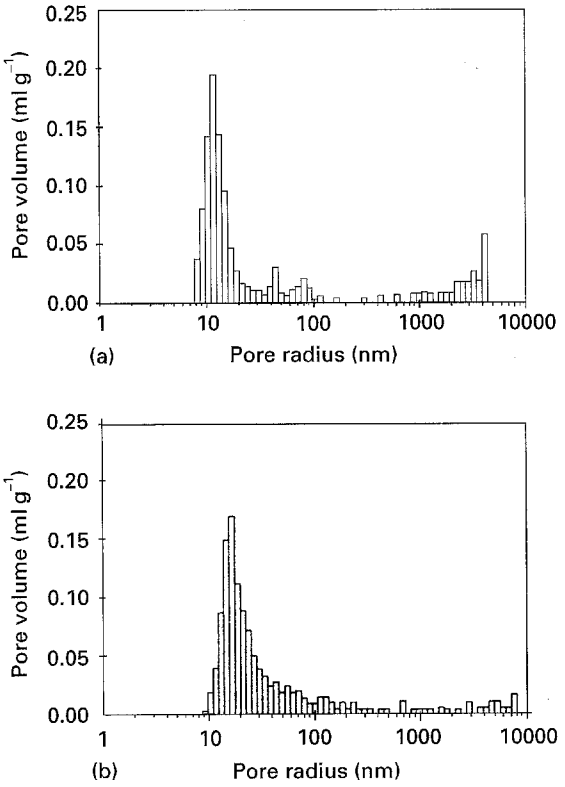

Figure 3 Pore-size distribution of (a) Daiichi (I) and (b) Daiichi (II) materials treated in air at 850 °C for 16 h as determined by mercury intrusion porosimetry.

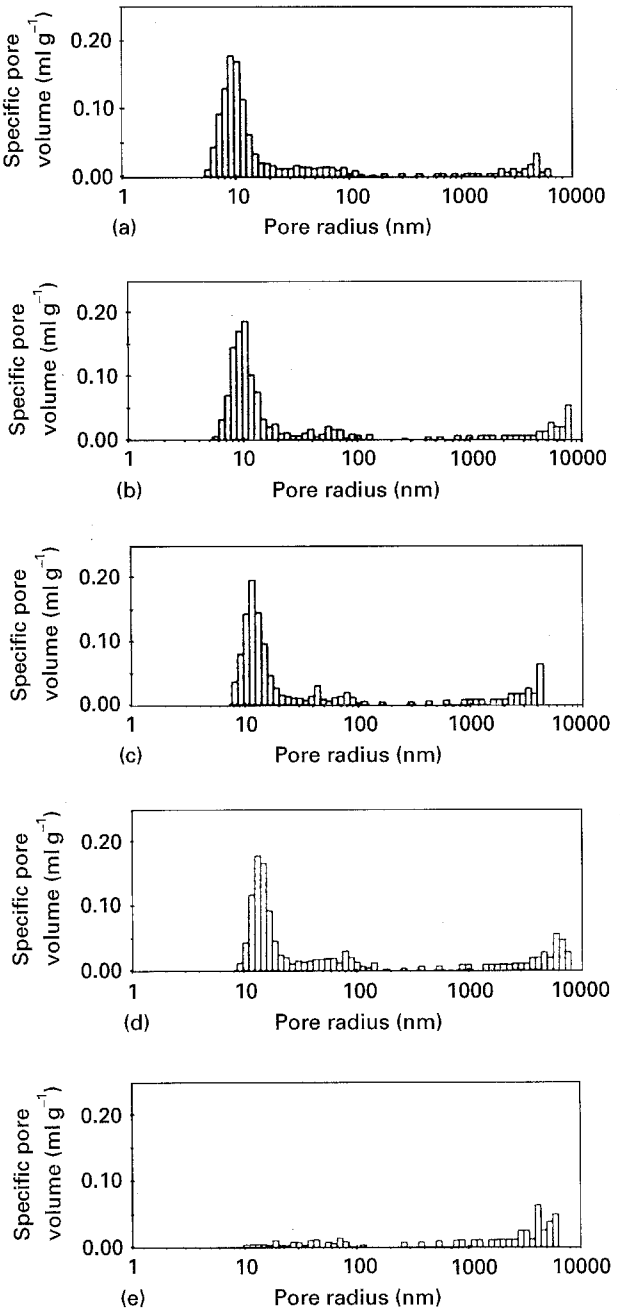

Figure 4 Evolution of pore-size distribution of the fresh Daiichi (I) material with the temperature of thermal treatment in air for 16 h as determined by mercury intrusion porosimetry. (a) Fresh, (b) 700 °C, (c) 800 °C, (d) 900 °C, (e) 1100 °C.

treatment (Fig. 4), the median pore radius of the population of small pores shifts to higher values, but the total porosity does not change significantly. At 1100 °C, the small pores are eliminated and only the large macropores remain.

Steam treatment seems to affect the texture of the zirconia in a different way from thermal treatment in dry air at the same temperature (Table V). The zirconia support shows a surface area after treatment with steam which is lower than the surface area to be expected after heating in dry air (cf. Fig. 2). Probably the surface diffusion of ions necessary for sintering is enhanced by the presence of steam. However, when a sample is pre-treated in air, no additional decrease in surface area can be observed. Even after 64 h, no large effect on the surface area or porosity is observed. Also the autoclave experiments do not show a significant influence of the water vapour on the zirconia support. After 64 h treatment, the decrease in specific area is only 1 $m^2 g^{-1}$. Moreover, with XRD the formation of other phases, for example, zirconium hydroxides, has not been observed after applying hydrothermal conditions.

3.4. Powder X-ray diffraction

X-ray diffractograms of the fresh supports are represented in Fig. 5. It can be seen that the Daiichi and Norton supports are purely monoclinic, whereas the Engelhard support is a mixture of the tetragonal and monoclinic polymorph.

The evolution of the crystallite sizes with the treatment temperature as calculated from XRD was also determined (Fig. 6). For the Daiichi (I) material, the crystallite radii in the fresh (8 nm) and in the thermally treated (850 °C, 15 nm) samples show a reasonable agreement with the upper limit of the crystallite sizes observed with TEM. This indicates that in the weight–mean average particle size, the larger crystallites constitute the majority. Furthermore, the fact that the crystallite radii determined from different diffraction lines do agree well (Fig. 6) suggests that the zirconia crystallites are isomorphic. This also is in agreement with the TEM images.

From the geometrical surface, S_{geo}, calculated from the crystallite radius, the fraction of the surface inaccessible for gas molecules can be determined by dividing the difference of S_{geo} and the specific surface

TABLE V Textural parameters of zirconia supports after 16 h steam treatment. For explanation of symbols see Table III

Treatment	Support	SSA ($m^2 g^{-1}$)	PV ($ml g^{-1}$)	$\langle r \rangle$ (nm)	ε (%)	S_μ ($m^2 g^{-1}$)
600 °C/30% steam	Daiichi I, treated at 850 °C	20.6	0.17	16.8	50	3.0
700 °C/30% steam	Daiichi II					
	fresh	20	0.20	21.2	53	4.2
	treated at 850 °C	18	0.18	20.2	50	4.0

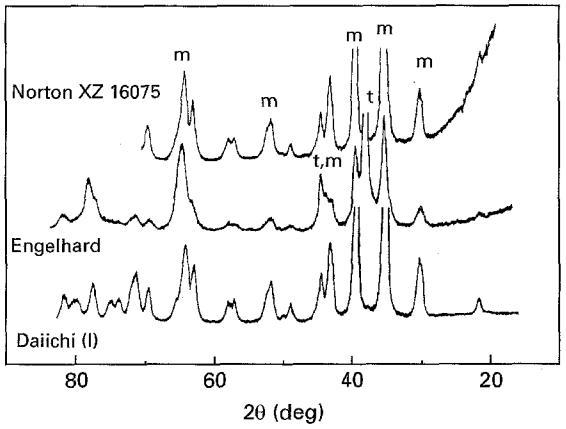

Figure 5 Powder diffractograms of various fresh zirconia supports.

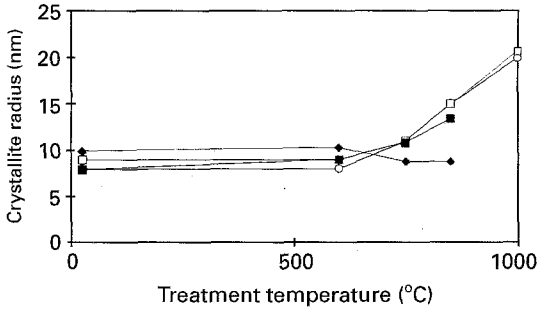

Figure 6 Evolution of the zirconia crystallite radii for the Daiichi (I) and Engelhard materials as a function of the temperature of thermal treatment in air for 16 h. (□, ○) Daiichi; (■,◆) Engelhard. Calculated from: (□) m-(1 1 1); (○) m-(1 1 $\bar{1}$); (◆) t-(1 1 1).

area SSA by S_{geo}

$$f_{in}(\%) = (S_{geo} - SSA)/S_{geo} \times 100\% \quad (2)$$

From these calculations, it follows that this inaccessible fraction hardly increases with the applied thermal treatment: 41% after thermal treatment versus 40% for the fresh support. This indicates that interparticle sintering does not proceed very rapidly with these samples at this temperature. When the same calculations are performed for powdered materials [9], a value of 84% is obtained. This is reflected by the much lower porosity of the powdered samples (5%) after treatment at 850 °C, which might be a result of the crystallites being in closer contact.

The behaviour of the Engelhard support is typical for a mixture of monoclinic and tetragonal crystallites [10]. By conversion of an increasing fraction of the metastable tetragonal phase into the monoclinic phase (Fig. 7), the t-crystallite sizes calculated from XRD remain approximately constant (Fig. 6). This can be

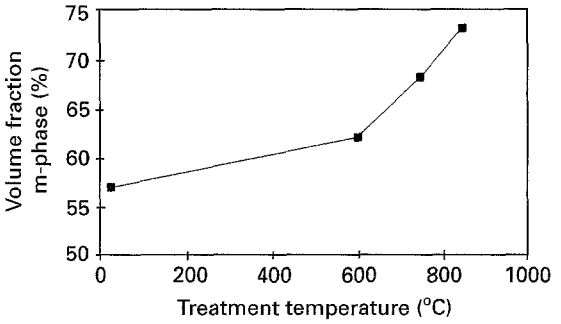

Figure 7 Evolution of the monoclinic phase volume fraction of the Engelhard material as calculated from XRD as a function of the temperature of thermal treatment in air for 16 h.

understood when realizing that any t-crystallite growing to a size exceeding the critical crystallite size transforms into an m-crystallite. The m-crystallite size increases at roughly the same rate as in the purely monoclinic Daiichi support. The inaccessible fraction of the surface area increases more extensively in the Engelhard material. An increase from 25% to 55% can be calculated from the combined data of the monoclinic and the tetragonal phases. This indicates a more extensive interparticle sintering behaviour. This was already observed in TEM: the large agglomerates were denser after thermal treatment.

4. Further discussion and conclusion

The aim of this study was to gain knowledge on the important properties of various pre-shaped zirconia supports, in order to determine the suitability of the supports for use in dehydrogenation catalysts. The properties studied here were the thermostability, the stability against steam, and structural properties. The chemical properties involved, such as the behaviour of the support towards iron and potassium, the main constituents of a dehydrogenation catalyst, will be described in a forthcoming paper.

As could be expected from the literature, zirconia is sufficiently thermostable to be used as a support. Specific surface areas up to $10 m^2 g^{-1}$ are stable up to temperatures as high as 850 °C, which should be adequate for the catalytic dehydrogenation: proven bulk iron oxide catalysts for the dehydrogenation reaction usually have a smaller surface area. Specific surface areas up to about $30 m^2 g^{-1}$ can be installed by a thermal treatment in air. Steam treatment affects the texture differently from treatment in dry air: sintering proceeds more rapidly.

The pre-shaped supports studied here show a porosity which is higher than is reported for zirconia

powders with the same pore-size distribution. This is advantageous, both in the catalyst preparation step and in the catalytic reaction. When catalysts are prepared by incipient wetness impregnation, it is convenient that the supports have a reasonably large pore volume, because the precursor for the active phase has to be dissolved in this fixed volume of solvent. The larger the pore volume, the more parameters (*e.g.* precursor concentration, precursor compound) can (in principle) be varied for optimizing catalyst preparation. However, the supports show a rather high microporosity. To what extent the micropores influence the performance in the dehydrogenation reaction is yet unknown and will become apparent in catalyst characterization and catalytic studies.

The drawbacks of magnesia, which were mentioned in the introduction, do not apply to zirconia: after a steam treatment, no hydroxides or extra microporosity was observed. It is therefore concluded that zirconia is a promising support material for the development of a supported dehydrogenation catalyst system, based on the investigated pre-shaped support bodies.

Acknowledgements

L. B. thanks P. A. Elberse for the texture analysis measurements and B. G. Dekker for helpful discussions.

References

1. B. D. HERZOG and H. F. RASE, *Ind. Eng. Chem. Prod. Res. Dev.* **23** (1984) 187.
2. P. G. MENON, *Chem. Rev.* **94** (1994) 1021.
3. D. E. STOBBE, F. R. VAN BUREN, A. J. VAN DILLEN and J. W. GEUS, *J. Catal.* **135** (1992) 533.
4. *Idem, ibid.* **135** (1992) 548.
5. D. E. STOBBE, F. R. VAN BUREN, P. E. GROENENDIJK, A. J. VAN DILLEN and J. W. GEUS, *J. Mater. Chem.* **1** (1991) 539.
6. D. E. STOBBE, PhD thesis, Utrecht University (1990).
7. L. A. BOOT, PhD thesis, Utrecht University, ISBN 90-393-0895-0 (1994).
8. E. H. LEE, *Catal. Rev.* **8** (1973) 285.
9. P. D. L. MERCERA, PhD thesis, Technical University Twente, ISBN 90-900-4189-3 (1991).
10. P. D. L. MERCERA, J. G. VAN OMMEN, E. B. M. DOESBURG, A. J. BURGGRAAF and J. R. H. ROSS, *Appl. Catal.* **57** (1990) 127.
11. *Idem, ibid.* **71** (1991) 363.
12. K. TANABE and T. YAMAGUCHI, *Catal. Today* **20** (1994) 185.
13. I. WANG, W. F. CHANG, R. H. SHIAU, J. C. WU and C. S. CHUNG, *J. Catal.* **83** (1983) 428.
14. L. A. BOOT, S. C. VAN DER LINDE, A. J. VAN DILLEN, J. W. GEUS, F. R. VAN BUREN and J. E. BONGAARTS, in "Studies on Surface Science of Catalysts", Vol. 88, Catalyst Deactivation VI, edited by B. Delmon and G. Froment (Elsevier, Amsterdam, 1994) p. 491.
15. H. VON WARTENBERG and W. GURR, *Z. Anorg. Allg. Chem.* **196** (1931) 374.
16. T. S. JONES, S. KIMURA and A. MUAN, *J. Am. Ceram. Soc.* **50** (1967) 137.
17. G. MAREST, C. DONNET and J. A. SAWICKI, *Hyperfine Interact.* **56** (1990) 1605.
18. J. F. COLLINS and I. F. FERGUSON, *J. Chem. Soc. (A)* (1968) 4.
19. S. DAVISON, R. KERSHAW, K. DWIGHT and A. WOLD, *J. Solid State Chem.* **73** (1988) 47.
20. J. G. VAN OMMEN, H. BOSCH, P. J. GELLINGS and J. R. H. ROSS, in "Studies on Surface Science of Catalysts", Vol. 31, Preparation of Catalysts IV, edited by B. Delmon, P. Grange, P. A. Jacobs and G. Poncelet (Elsevier, Amsterdam, 1987) p. 151.
21. E. GUGLIELMINOTTI, *J. Phys. Chem.* **98** (1994) 4884.
22. H. A. LEHMANN and P. ERZBERGER, *Z. Anorg. Allg. Chem.* **301** (1959) 233.
23. P. HAGENMULLER and M. TOURNOUX, *Compt. Rend. (Paris)* **253** (1961) 465.
24. M. TOURNOUX, *Rev. Hautes Temp. Réfract.* **1** (1964) 343.
25. T. A. VALASANYAN and R. K. ALIEV, *Kinet. Catal.* **31** (1990) 212.
26. H. Th. RIJNTEN, PhD thesis, Delft University of Technology (1971).
27. S. LOWELL and J. E. SHIELDS, "Powder Surface Area and Porosity", 2nd edn (Chapman and Hall, London, 1984).
28. H. TORAYA, M. YOSHIMURA and S. SOMIYA, *J. Am. Ceram. Soc.* **67** (1984) C-119.

Received 8 August
and accepted 21 December 1995